Original Paper

Integrating Quantitative Morphological and Intratumoural Textural Characteristics in FDG-PET for the Prediction of Prognosis in Pharynx Squamous Cell Carcinoma Patients

Abbreviations

3D: three-dimensional, AUC: area under the curve, CI: confidence interval, CT: computed tomography, CV: coefficient of variance, FDG: ^{18}F-fluorodeoxyglucose, FOV: field of view, FWHM: full width at half maximum, GLCM: gray-level co-occurrence matrix, HNSCC: head and neck squamous cell carcinoma, HPV: human papillomavirus, HR: hazard ratio, MRI: magnetic resonance imaging, MTV: metabolic tumour volume, NPV: negative predictive value, OS: overall survival, PET: positron-emission tomography, PFS: progression-free survival, PPV: positive predictive value, ROC: receiver operating characteristic, ROI: region of interest, SUV: standard uptake value, TLG: total lesion glycolysis, VIF: variance inflation factor

ABSTRACT

Aim: We assessed potential prognostic factors in pharynx squamous cell carcinoma (SCC) patients by quantitative morphological and intratumoural characteristics obtained by ^{18}F-fluorodeoxyglucose positron-emission tomography/computed tomography (FDG-PET/CT).

Materials and Methods: We retrospectively analyzed the cases of 54 patients with pharynx SCC who underwent chemoradiation therapy. Using their FDG-PET data, we calculated the quantitative morphological and intratumoural characteristics of 14 parameters. The progression-free survival (PFS) and overall survival (OS) information was obtained from patient medical records. We performed univariate and multivariate analyses to assess the 14 quantitative parameters as well as the T-stage, N-stage and tumour location data for their relation to PFS and OS. When an independent predictor was suggested in the multivariate analysis, the parameter was further assessed by the Kaplan-Meier method.

Results: In the assessment of PFS, the univariate and multivariate analyses indicated the following as independent predictors: the texture parameter of homogeneity, and the morphological parameter of sphericity. In the Kaplan-Meier analysis, the PFS rate was significantly improved in the patients who had both a higher value of homogeneity

(p=0.01) and a higher value of sphericity (p=0.002). With the combined use of homogeneity and sphericity, we could divide the patients with different PFS rates more clearly.

Conclusion: The quantitative parameters of homogeneity and sphericity obtained by FDG-PET can be useful for the prediction of the PFS of pharynx SCC patients, especially when used in combination.

1. Introduction

In patients with head and neck squamous cell carcinoma (HNSCC), the selection of the treatment method is generally based on the location of the primary site and TNM (tumour, node, metastasis) staging. Patients with advanced cases of oropharyngeal or hypopharyngeal SCC commonly undergo nonsurgical treatments such as chemotherapy, radiotherapy, and combinations of these approaches. [1]. For such nonsurgical therapies, it is important to predict the treatment outcome, as being able to do so will contribute to the optimization of patient management (including the selection of additional treatment and/or follow-up strategy).

For the evaluation of HNSCC with a primary site in the oropharynx or hypopharynx, positron-emission tomography (PET) with ^{18}F-fluorodeoxyglucose (FDG, which depicts a tumour's rate of glucose metabolism) has been a major diagnostic modality. The tumour metabolic rate is one of the important factors that reflect tumour aggressiveness [2, 3]. In particular, an FDG-PET/computed tomography (FDG-PET/CT) scanner is used in most institutions for the clinical assessment. FDG-PET/CT can provide not only tumour metabolic information but also anatomical information with the use of PET-CT fusion imaging. Several studies have investigated FDG-PET parameters in HNSCC patients, examining mainly the maximum standard uptake value (SUVmax),

the metabolic tumour volume (MTV), and the total lesion glycolysis (TLG) for the prediction of treatment outcomes as a prognostic factor in HNSCC [4–6]. However, in those reports, the diagnostic power was not sufficient and there was a certain degree of overlap between the patients with good prognoses and those with poor prognoses.

As another approach for the evaluation of FDG uptake, the utility of textural parameters of FDG distribution in HNSCC was reported [7–10]. This method has the advantage of being an objective method of measuring tumour heterogeneity in greater detail, and such textural parameters may predict treatment outcomes with high diagnostic accuracy. However, the number of studies that have investigated the textural features of HNSCC in FDG-PET images is very limited.

In contrast, as mentioned above, FDG-PET/CT data also provide anatomical information. Although the details of a tumour's anatomical information can be revealed by using CT or magnetic resonance imaging (MRI), conventional CT and MRI are affected by the ability of the individual clinician who outlines the tumour region of interest (ROI). In addition, with conventional CT or MRI, it is difficult to outline a tumour with a completely automated method because a clear discrimination between the tumour and the surrounding tissue is sometimes difficult to obtain due to the varying density and/or signal intensity of surrounding tissue by inflammatory change or tissue

edema. In contrast, it is relatively easy to set a tumour's margin on an FDG-PET image by using a threshold FDG uptake value, and this method can be used to objectively determine the entire tumour area [11]. It has been noted that a tumour's three-dimensional (3D) shape can be semiquantitatively determined by using several anatomical parameters, and these parameters were reported to be useful for the prediction of treatment outcomes in head and neck cancers; however, the number of studies that have conducted such a tumour shape analysis is also very limited [12, 13].

In the present study, we investigated the tumour characteristics (i.e., anatomical shape and intratumoural features) in patients with pharynx cancer by a completely automated method using the patients' pre-treatment FDG-PET images. We also assessed the diagnostic value of the integrated use of these characteristics for the prediction of the patients' progression-free survival (PFS) and overall survival (OS) rates.

2. Materials and Methods

2.1. Patients

The protocol of this retrospective study was approved by our institutional review board, and written informed consent from the patients was waived. The 54 patients who were referred to our hospital and underwent chemoradiation treatment under a diagnosis of

oropharynx or hypopharynx SCC in the period from September 2009 to November 2013 and who met the following inclusion criteria were enrolled: (1) the histopathological diagnosis was SCC; (2) the patient underwent a full course of curative chemoradiation treatment with a radiation dose of 65–70 Gy; and (3) FDG-PET/CT was performed before any treatment. The treatment regimen was chemoradiation therapy with curative intent for all patients. The treatment details were as follows: systemic chemotherapy with weekly cisplatin (40 mg/m^2 per wk for 3–5 wks) with concurrent radiotherapy of total 65–70 Gy.

Among the total series of 54 patients, 22 patients underwent induction chemotherapy with 1–3 cycles of docetaxel, cisplatin and 5-fluorouracil. Generally, patients with a primary site considered resectable and appropriate for surgical treatment (mainly early stage such as T1 or T2) were treated by surgery; such patients were thus excluded from this study. Decisions regarding treatment methods were based on consensus among head-and-neck surgeons and radiation oncologists following the Japanese clinical practice guidelines for head and neck cancer. None of the patients in the study underwent surgical treatment at the primary site.

2.2. Clinical assessment

Using the patients' medical records, we determined the OS and PFS durations of all patients in the individual follow-up periods after curative treatment. For the OS assessment, we defined OS as the survival period up to the patient's death due to his/her cancer or to any other causes. For the PFS assessment, we defined progressive disease as primary tumour progression or the progression of distant metastatic or lymph node metastasis. The patients were followed up by visual inspection by fiberscopy, radiological assessment in CT and MRI with the scan interval of 3–12 months, and/or PET/CT with the scan interval of 6–12 months, according to the follow-up protocol of our institution.

2.3. Imaging protocol

FDG-PET/CT images were acquired with a Biograph 64 PET/CT scanner (Asahi-Siemens Medical Technologies, Tokyo). The patient fasted for ≥6 hr before the injection of FDG (4.5 MBq/kg) and waited 60 min post-injection. All patients were instructed to sit as calmly as possible, and not to talk. The patients with a pre-scanning blood glucose measurement >200 mg/dL were excluded from further analysis. The energy window was 425–650 keV. The transaxial and axial fields of view (FOVs) were 58.5 cm and 21.6 cm, respectively. A 3-min emission scanning in 3D mode was

performed for each bed position. Attenuation was corrected with CT images acquired without contrast media.

The images were reconstructed with an iterative method integrated with a point spread function (TrueX) [14]. Fully 3D-PET reconstruction with a system matrix derived from point source measurements was conducted. The reconstructed image had a spatial resolution of 8.4 mm full width at half maximum (FWHM) and a matrix size of 168×168 with a voxel size of 4.1×4.1×2.0 mm. The SUV was defined as the tissue concentration of radioactivity (kBq/mL) divided by the injected dose per body weight (kBq/g), as is commonly used [15].

2.4. Image analysis

For the quantitative evaluation of the FDG uptake in the primary tumour, we estimated both the morphological and intra-tumoural characteristics. We measured the SUV value for each tumour by determining the automated ROI using an isocontour threshold method. A threshold SUV value of 2.5 was set for the tumour ROI delineation to exclude the central necrosis or nearly normal tissue uptake [16]. If a tumour extended to two or more slices, all slices that showed tumour FDG uptake were analyzed.

For the analysis of morphological characteristics, we calculated the tumour

volume and tumour surface area from the morphological shape of all selected tumour voxels with an SUV value >2.5. The sphericity and irregularity of each tumour were also calculated by the following equations [17]:

$$Sphericity = \frac{TV}{(1/6) * \sqrt{\frac{TSA^3}{\pi}}} \quad (1)$$

$$Irregularity = 1 - \frac{4\pi * (\frac{3TV}{TSA})^{\frac{2}{3}}}{TSA} \quad (2)$$

where TV is the tumour volume, and TSA is the tumour surface area. When the TV was the value of V mL, and TSA was the value of S cm^2 in a given case, the sphericity represents the actually measured tumour volume V mL divided by the calculated volume of the sphere whose surface area was S cm^2, as shown by Eq. (1). The irregularity indicates the value of the calculated surface area of the sphere whose volume was V mL divided by the actually measured tumour surface area S cm^2, and this value is then subtracted from 1, as shown by Eq. (2).

For the intra-tumoural characteristics analysis, we calculated the SUVmean, SUVmax, the histogram, and textural parameters within the ROI. The histogram features included the coefficient of variance (CV), kurtosis, and skewness. Textural

features included the contrast, correlation, energy, and homogeneity, which we calculated based on the gray-level co-occurrence matrix (GLCM) features. The GLCM features are the spatially detailed information of signal intensity in the tumour ROI, compared to the histogram parameters. The GLCM is composed of the square plane with rows and columns from zero to the maximum value of the gray scale in the tumour ROI. The GLCM element in row *i* and column *j* represents the number of times a given gray tone of value *i* is horizontally adjacent to a gray tone *j* in the original quantized image. For simplicity, we calculated the GLCMs by using only directly adjacent pixels. The details of GLCM features and the calculation details including the equation were as described [18, 19]. We calculated the TLG by multiplying the tumour volume and the SUVmean value.

Finally, all parameters of morphological features, SUVmax, SUVmean, histogram parameters, textural parameters, and TLG were calculated for each tumour. We used the self-developed program by MATLAB ver. 2012a (MathWorks, Natick, MA) for the above-described calculations.

2.5. Statistical analysis

For the assessment of PFS, we first conducted a univariate analysis to analyze the age,

T-stage, N-stage, presence of induction chemotherapy, and all obtained FDG-related parameters, using the univariate Cox regression model. When a significant difference was observed in more than two parameters, these parameters were further analyzed by a multivariate Cox regression analysis. Hazard ratios (HRs) and corresponding 95% confidence intervals (CIs) were calculated. In the multivariate analysis, multicollinearity between respective parameters was assessed in advance with the variance inflation factors (VIFs) (reference value of 10) before the final output to the multivariate analysis.

If at least one parameter was determined as an independent predictor in the multivariate Cox regression analysis, that parameter was subsequently assessed in a receiver operating characteristic (ROC) curve analysis and a Kaplan-Meier curve analysis. In the ROC curve analysis, we calculated the optimal cut-off value by using the closest point to the upper left corner of the ROC curve in the division of patients with progression-free status (non-local relapse and non-distant metastasis) within the whole follow-up period and those without, and we also calculated the sensitivity, specificity, positive and negative predictive values, and accuracy.

In the Kaplan-Meier curve analysis, we divided the patients into two groups by using the cut-off value obtained in the ROC curve analysis. The PFS rates between these

two groups were calculated and compared by the log-rank test. P-values <0.05 were considered significant in these analyses. In addition, if more than two parameters were revealed as significant predictors by the log-rank test in the Kaplan-Meier analysis, a further additional analysis was performed as follows; by using all of the significant parameters' cut-off values, we also performed a Kaplan-Meier curve analysis under the combination of cut-off values with the patients divided into three groups: the all-parameters-negative group, the ≥1-parameter-positive group, and the all-parameters-positive group. In this analysis, a Bonferroni-corrected p-value <0.05 was accepted as significant.

In the OS assessment, the same analyses as those described above for PFS were performed with the division of patients into those with survival status (i.e., alive) within the follow-up period and those without survival status. SPSS software (IBM, Armonk, NY) was used for all analyses.

3. Results

All FDG-PET/CT scanning was successfully performed without severe artifacts. The 54 patients' pre-scanning blood glucose ranged from 71 to 134 mg/dL (median, 101 mg/dL). The characteristics of all patients are summarized in Table 1. Of the total series of 54

patients, 19 were without progression-free status (i.e., local relapse and/or distant metastasis was present in the follow-up period), and 10 patients were without survival status (i.e. they died during the follow-up period), based on their medical records including the histological diagnosis with biopsy, visual inspection and radiological findings during the follow-up period. The median follow-up period for the group of 35 patients who were progression-free during the follow-up period was 49.5 months (range 18–78 months), and that of the 44 patients who were survivors during the follow-up period was 49.8 months (range 18–78 months).

3.1. Assessment of PFS

The univariate Cox regression analysis for PFS revealed the following as significant parameters: contrast, homogeneity, sphericity, and irregularity. In the multivariate Cox regression analysis, both homogeneity and sphericity were identified as independent predictors of PFS. The details of these analyses are provided in Table 2. The cut-off values were determined by the ROC curve analysis for the division of patients with and without progression-free status in the follow-up period (Table 3).

In the Kaplan-Meier analysis, the PFS rate was significantly greater in both the group of patients with lower values of homogeneity ($p=0.01$) and the patient group with

higher values of sphericity (p=0.002). With the combined use of homogeneity and sphericity, the PFS rate could be divided more clearly. The detectability of longer-PFS patients with the combination of high homogeneity and high sphericity in particular was improved, and the detectability of shorter-PFS patients with low homogeneity and low sphericity was sufficient compared to the use of either single parameter. All of the results of the Kaplan-Meier analyses are illustrated in Figure 1.

3.2. Assessment of OS

The univariate Cox regression analysis for OS revealed the following as significant parameters: contrast, homogeneity, sphericity, and irregularity. However, in the multivariate analysis, no parameter was shown to be an independent predictor of OS, and therefore, no further analysis was performed for OS. The details of these analyses are given in Table 4.

4. Discussion

Our analyses demonstrated that the quantitative morphological parameter of sphericity and the intra-tumoural characteristic of homogeneity were independent predictors of the PFS in patients with oropharyngeal and hypopharyngeal SCC who have undergone

chemoradiation therapy with curative intent. Notably, the combined use of tumour homogeneity and morphological sphericity indicated its potential as a useful clinical tool. In addition, the parameter calculation can be performed by a semi-automated method, and thus parameter estimations can be accomplished easily regardless of the level of operator experience.

We observed that the quantitative characteristic sphericity of the tumour (morphological information) is a significant predictor. As is generally well known, the shapes of HNSCCs show several patterns. Some HNSCCs progress in an expanding pattern rather than invading to the deep area under the mucosa; this pattern was described as related to human papillomavirus (HPV) status-positive SCCs [20], and it is likely to be related to the good prognosis. In contrast, several HNSCCs progress along the area of mucosa with invasion to the deep area rather than expanding. Such tumours have complicated shapes and a large surface area considering their volume. We suspect that the prognosis of such tumours will be worse, because the gross tumour volume will take a complicated shape and it may be difficult to adapt the radiation field to such complicated shapes without the elevation of other organs' radiation dose.

FDG-PET can easily visualize the rough shape of such anatomically complicated tumours automatically, when a chosen SUV threshold is set. By using a quantitative

parameter such as the sphericity, we can easily assess the tumour morphological information as an objective index, i.e., as a quantitative value. The number of studies that investigated tumour morphological features by using quantitative parameters and the SUV uptake is also very limited [12, 13], and the results of these studies indicated that tumours with high asphericity (i.e., low sphericity) are associated with poor prognosis. Our present findings indicate the same trend.

Our analyses also revealed tumour heterogeneity as a prognostic factor. Cheng et al. reported that the textural parameter of zone-size nonuniformity is an independent predictor of outcome in patients with advanced T-stage oropharyngeal SCC [7]. This parameter essentially reflects the textural feature of intra-tumoural heterogeneity. The parameter of homogeneity revealed by our present investigation might include the resembling characteristics to a degree compared to zone-size nonuniformity. We observed herein that the combined use of a quantitative morphological parameter (sphericity) and a texture heterogeneity parameter (homogeneity) may be useful for the estimation of a patient's prognosis using data from only one pretreatment FDG-PET scan in cases of curative chemoradiation therapy.

A report by Wang et al. demonstrated the usefulness of the combination of tumour texture heterogeneity parameters and the information of gene expression [8].

Chan et al. also concluded that multi-parametric imaging based on PET heterogeneity and dynamic contrast-enhanced MRI parameters combined with clinical risk factors was a useful diagnostic tool for the prediction of patient prognosis [10]. We speculate that the combined use of all of these characteristics as well as the combined use of the tumour morphological and textural features could be a strong prognostic tool, but further studies are needed to test this idea.

Unlike our study's PFS assessment, in the assessment of OS, although several FDG parameters were suggested to be related to the patient OS in the univariate analysis, no significance was observed in the multivariate analysis. We suspect that the reason for this was that the group of patients without OS included other causes of death that occurred during the follow-up period (e.g., eventual cardiac disease or other types of cancer). Such causes of death can be difficult to predict based on only the FDG characteristics of patients' primary HNSCCs. The small number of patients without OS (n=10) may also have affected this result.

Our study has several limitations. First, the patient number was quite small, and the study's design was retrospective. We thus did not perform a validation study. A further validation study is strongly required to confirm the clinical utility indicated by our present findings. Second, the treatment methods were not completely homogeneous;

several patients underwent induction chemotherapy before the full course of chemoradiotherapy. Moreover, both oropharynx and hypopharynx cancers were included and analyzed. However, from the results of the univariate and multivariate analyses, we believe that the present results can be used regardless of the treatment details as long as the treatment regimens are curative, and they can also be used in both oropharyngeal and hypopharyngeal SCC patients. Third, the correlation data of the patients' HPV status were unknown. Unfortunately, most of the patients had not undergone an analysis of their HPV status.

In conclusion, a quantitative evaluation of morphological and intratumoural characteristics was successfully performed. Both higher sphericity and higher homogeneity were revealed as predictors of the patient PFS status. This quantitative method of FDG-PET and the combined use of the morphological and intratumoural characteristics can become a useful tool for the determination of additional treatment or follow-up strategies in patients with oropharyngeal and hypopharyngeal SCC who have undergone chemoradiation therapy with curative intent.

References

1. Wong SJ, Harari PM, Garden AS, et al. Longitudinal Oncology Registry of Head and Neck Carcinoma (LORHAN): analysis of chemoradiation treatment approaches in the United States. Cancer. 2011;117(8):1679-1686.
2. Rohren EM, Turkington TG, Coleman RE. Clinical applications of PET in oncology. Radiology 2004;231(2):305-332.
3. Kitagawa Y, Sano K, Nishizawa S, et al. FDG-PET for prediction of tumour aggressiveness and response to intra-arterial chemotherapy and radiotherapy in head and neck cancer. Eur J Nucl Med Mol Imaging 2003;30(1):63-71.
4. Higgins KA, Hoang JK, Roach MC, et al. Analysis of pretreatment FDG-PET SUV parameters in head-and-neck cancer: tumor SUVmean has superior prognostic value. Int J Radiat Oncol Biol Phys 2012;82(2):548-553.
5. Taghipour M, Sheikhbahaei S, Marashdeh W, Solnes L, Kiess A, Subramaniam RM. Use of 18F-fludeoxyglucose-positron emission tomography/computed tomography for patient management and outcome in oropharyngeal squamous cell carcinoma: a review. JAMA Otolaryngol Head Neck Surg 2016;142(1):79-85.
6. Moon SH, Choi JY, Lee HJ, et al. Prognostic value of 18F-FDG PET/CT in

patients with squamous cell carcinoma of the tonsil: comparisons of volume-based metabolic parameters. Head Neck 2013;35(1):15-22.

7. Cheng NM, Fang YH, Lee LY, et al. Zone-size nonuniformity of 18F-FDG PET regional textural features predicts survival in patients with oropharyngeal cancer. Eur J Nucl Med Mol Imaging 2015;42(3):419-428.

8. Wang HM, Cheng NM, Lee LY, et al. Heterogeneity of (18)F-FDG PET combined with expression of EGFR may improve the prognostic stratification of advanced oropharyngeal carcinoma. Int J Cancer 2016;138(3):731-738.

9. Chen SW, Shen WC, Lin YC, et al. Correlation of pretreatment 18F-FDG PET tumor textural features with gene expression in pharyngeal cancer and implications for radiotherapy-based treatment outcomes. Eur J Nucl Med Mol Imaging 2017;44(4):567-580.

10. Chan SC, Cheng NM, Hsieh CH, et al. Multiparametric imaging using 18F-FDG PET/CT heterogeneity parameters and functional MRI techniques: prognostic significance in patients with primary advanced oropharyngeal or hypopharyngeal squamous cell carcinoma treated with chemoradiotherapy. Oncotarget 2017;8(37):62606-62621.

11. Fruehwald-Pallamar J, Czerny C, Mayerhoefer ME, et al. Functional imaging in

head and neck squamous cell carcinoma: Correlation of PET/CT and diffusion-weighted imaging at 3 Tesla. Eur J Nucl Med Mol Imaging 2011;38(6):1009-1019.

12. Apostolova I, Steffen IG, Wedel F, et al. Asphericity of pretherapeutic tumour FDG uptake provides independent prognostic value in head-and-neck cancer. Eur Radiol 2014;24(9):2077-2087.

13. Hofheinz F, Lougovski A, Zophel K, et al. Increased evidence for the prognostic value of primary tumor asphericity in pretherapeutic FDG PET for risk stratification in patients with head and neck cancer. Eur J Nucl Med Mol Imaging 2015;42(3):429-437.

14. Panin VY, Kehren F, Michel C, Casey M. Fully 3-D PET reconstruction with system matrix derived from point source measurements. IEEE Trans Med Imaging 2006;25(7):907-921.

15. Sato J, Kitagawa Y, Yamazaki Y, et al. Advantage of FMISO-PET over FDG-PET for predicting histological response to preoperative chemotherapy in patients with oral squamous cell carcinoma. Eur J Nucl Med Mol Imaging 2014;41(11):2031-2041.

16. Fujima N, Sakashita T, Homma A, et al. Glucose metabolism and its

complicated relationship with tumor growth and perfusion in head and neck squamous cell carcinoma. PLoS One 2016;11(11):e0166236.

17. Dhara AK, Mukhopadhyay S, Saha P, Garg M, Khandelwal N. Differential geometry-based techniques for characterization of boundary roughness of pulmonary nodules in CT images. Int J Comput Assist Radiol Surg 2016;11(3):337-349.

18. Dang M, Lysack JT, Wu T, et al. MRI texture analysis predicts p53 status in head and neck squamous cell carcinoma. AJNR Am J Neuroradiol 2015;36(1):166-170.

19. Haralick RM, Shanmugam K, Dinstein I. Textural features for image classification. IEEE Trans Syst Man Cybern 1973;3:610–621.

20. Cantrell SC, Peck BW, Li G, Wei Q, Sturgis EM, Ginsberg LE. Differences in imaging characteristics of HPV-positive and HPV-Negative oropharyngeal cancers: a blinded matched-pair analysis. AJNR Am J Neuroradiol 2013;34(10):2005-2009.

Table Captions and Figure Legends

Table 1. Patient characteristics (n=54)

Table 2. Patient characteristics and parameters for the assessment of PFS

[Table 2 footnote] The numbers of patients are provided in the Patient Characteristics column (except for age). Data are mean ± standard deviation in image parameters. *Significant difference. PFS: progression free survival, SUV: standard uptake value, CV: coefficient of variance, TLG: total lesion glycolysis, HR: hazard ratio, 95% CI: 95% confidence intervals, ‘excluded (multicollinearity)’: This parameter was excluded from the multivariate analysis because of its multicollinearity to other parameters.

Table 3. ROC analysis results

[Table 3 footnote] PFS: progression-free survival, AUC: area under the curve, PPV: positive predictive value, NPV: negative predictive value.

Table 4. Patient characteristics and parameters for the assessment of OS

[Table 4 footnote] The numbers of patients are provided in the Patient Characteristics column (except for age). Data are mean ± standard deviation in image parameters. *Significant difference. SUV: standard uptake value, CV: coefficient of variance, TLG: total lesion glycolysis, HR: hazard ratio, 95% CI: 95% confidence intervals, 'excluded (multicollinearity)': This parameter was excluded from the multivariate analysis because of its multicollinearity to other parameters.

Fig. 1. Results of the Kaplan-Meier analysis. The results of the Kaplan-Meier analysis for the calculation of: (**a**) PFS by homogeneity, (**b**) PFS by sphericity, and (**c**) PFS by the combination of homogeneity and sphericity.

Table 1. Patient characteristics (n=54)

	Number of patients
Age	
Range	39-76
Median	61
Average	60
Gender	
Male	46
Female	8
Primary tumor site	
Oropharynx	31
Hypopharynx	23
T-stage	
T1	6
T2	19
T3	17
T4a	10
T4b	2
N-stage	
N0	7
N1	8
N2a	3
N2b	24
N2c	8
N3	4

Table 2. Patient characteristics and parameters of the patients with and without PFS

			The presence of progression free status in the follow-up		Univariate analysis		Multivariate analysis	
			(+)	(–)	p-value	HR (95% CI)	p-value	HR (95% CI)
Patients' characte-ristics	Age	median (range)	62 (45-76)	58 (39-76)	0.85	0.98 (0.95, 1.02)		
	T-stage	T1	4	2	0.17	1.16 (0.91, 1.26)		
		T2	17	2				
		T3	9	8				
		T4	5	7				
	N-stage	N0	4	3	0.41	1.06 (0.71, 1.58)		
		N1	5	3				
		N2	25	10				
		N3	1	3				
	Location	oropharynx	21	10	0.81	0.98 (0.93, 1.11)		
		hypo-pharynx	14	9				
	Induction chemo-therapy	performed	14	8	0.74	0.96 (0.92, 1.13)		
		not performed	21	11				
Image parameters (parameter value)	SUV mean		6.7±1.4	7.6±1.6	0.24	1.31 (0.88, 1.71)		
	SUV max		17.4±7.4	20.3±6.4	0.39	1.14 (0.92, 1.29)		
	CV		0.46±0.12	0.55±0.11	0.14	1.56 (0.87, 2.2)		
	TLG (g)		108.3±92.9	160.7±109.7	0.27	1.36 (0.9, 1.73)		
	Skewness		0.98±0.32	1.03±0.45	0.91	1.01 (0.98, 1.04)		
	Kurtosis		3.15±0.89	3.46±1.48	0.74	0.97 (0.94, 1.02)		
	Contrast		8.9±4.6	16±7.9	0.03*	1.58 (1.32, 1.79)	excluded (multicollinearity)	
	Correlation		0.53±0.14	0.61±0.14	0.43	1.24 (0.84, 1.65)		
	Energy		0.058±0.093	0.031±0.03	0.38	1.18 (0.71, 1,68)		
	Homogeneity		0.43±0.07	0.37±0.05	0.02*	1.75 (1.1, 2.35)	0.02*	1.76 (1.13, 2.29)
	Tumor volume (cm^3)		12.6±10.9	20.2±12.6	0.16	1.13 (0.95, 1,38)		

Tumor surface area (cm^2)	48.7±27.8	83.5±41.8	0.09	2.12 (0.22, 6.79		
Sphericity	0.36±0.07	0.28±0.06	0.01*	2.35 (1.38, 4.05)	0.01*	2.71 (1.53, 4.66)
Irregularity	0.6±0.09	0.72±0.09	0.01*	2.32 (1.34, 3.99)	excluded (multicollinearity)	

Table 2 footnote: Number of patinets was provided in patients' characteristics except age. Data are mean ± standard deviation in image parameters. * indicate statistical significance. PFS: progression free survival, SUV: standard uptake value, CV: coefficient of variance, TLG: total lesion glycolysis, HR: hazard ratio, 95% CI: 95% confidence intervals, ‘excluded (multicollinearity)’ mean ‘this parameter was excluded in multivariate analysis because of its multicollinearity to other parameters’.

Table 3. ROC analysis results

Significant parameters in multivariate analysis for PFS assessment

Parameter	AUC	Sensitivity	Specificity	PPV	NPV	Accuracy	Cut-off value
Homogeneity	0.79	0.91	0.58	0.8	0.78	0.79	0.37
Sphericity	0.89	0.74	0.94	0.96	0.67	0.81	0.35

Table 3 footnote: PFS: progression free survival, AUC: area under curve, PPV: positive predictive value, NPV: negative predictive value

Table 4. Patient characteristics and parameters of the patients with and without OS

			The presence of survival status in the follow-up		Univariate analysis		Multivariate analysis	
			(+)	(–)	p-value	HR (95% CI)	p-value	HR (95% CI)
Patients' characte-ristics	Age	median (range)	65 (46-76)	60 (39-76)	0.77	0.96 (0.93, 1.02)		
	T-stage	T1	6	0	0.35	1.08 (0.95, 1.14)		
		T2	18	1				
		T3	14	3				
		T4	6	6				
	N-stage	N0	6	1	0.58	1.04 (0.96, 1.12)		
		N1	8	0				
		N2	28	7				
		N3	2	2				
	Location	oropharynx	27	4	0.86	0.99 (0.96, 1.04)		
		hypo-pharynx	17	6				
	Induction chemo-therapy	performed	18	4	0.89	0.98 (0.92, 1.06)		
		not performed	26	6				
Image parameters (parameter value)	SUV mean		6.8±1.5	7.9±1.3	0.85	1.01 (0.98, 1.04)		
	SUV max		17.7±7.2	21.3±6.4	0.75	1.05 (0.97, 1.12)		
	CV		0.48±0.12	0.53±0.1	0.19	1.42 (0.85, 2.11)		
	TLG (g)		103.5±108.7	174.8±116.3	0.23	1.33 (0.67, 2.28)		
	Skewness		1.01±0.39	0.95±0.24	0.94	1.01 (0.99, 1.02)		
	Kurtosis		3.26±1.22	2.95±0.56	0.82	1.02 (0.96, 1.08)		
	Contrast		10.2±5.8	16.5±8.5	0.04*	1.35 (1.25, 1.46)	excluded (multicollinearity)	
	Correlation		0.53±0.15	0.59±0.07	0.41	1.26 (0.74, 1.89)		
	Energy		0.055±0.05	0.021±0.00	0.46	1.19 (0.85, 1,48)		

	9	9				
Homogeneity	0.42±0.07	0.36±0.03	0.04*	1.57 (1.23, 1.85)	0.25	1.34 (0.73, 1.92)
Tumor volume (cm^3)	13.8±11.2	22.1±13.4	0.3	1.32 (0.75, 1,78)		
Tumor surface area (cm^2)	54.2±31.4	90.4±46.5	0.14	1.97 (0.34, 3.93		
Sphericity	0.36±0.07	0.28±0.06	0.02*	1.86 (1.41, 3.18)	0.36	1.48 (0.88, 2.14)
Irregularity	0.62±0.1	0.72±0.11	0.02*	1.84 (1.39, 3.12)	excluded (multicollinearity)	

Table 4 footnote: Number of patinets was provided in patients' characteristics except age. Data are mean ± standard deviation in image parameters. * indicate statistical significance. PFS: progression free survival, SUV: standard uptake value, CV: coefficient of variance, TLG: total lesion glycolysis, HR: hazard ratio, 95% CI: 95% confidence intervals, ‘excluded (multicollinearity)’ mean ‘this parameter was excluded in multivariate analysis because of its multicollinearity to other parameters’.

Fig1a

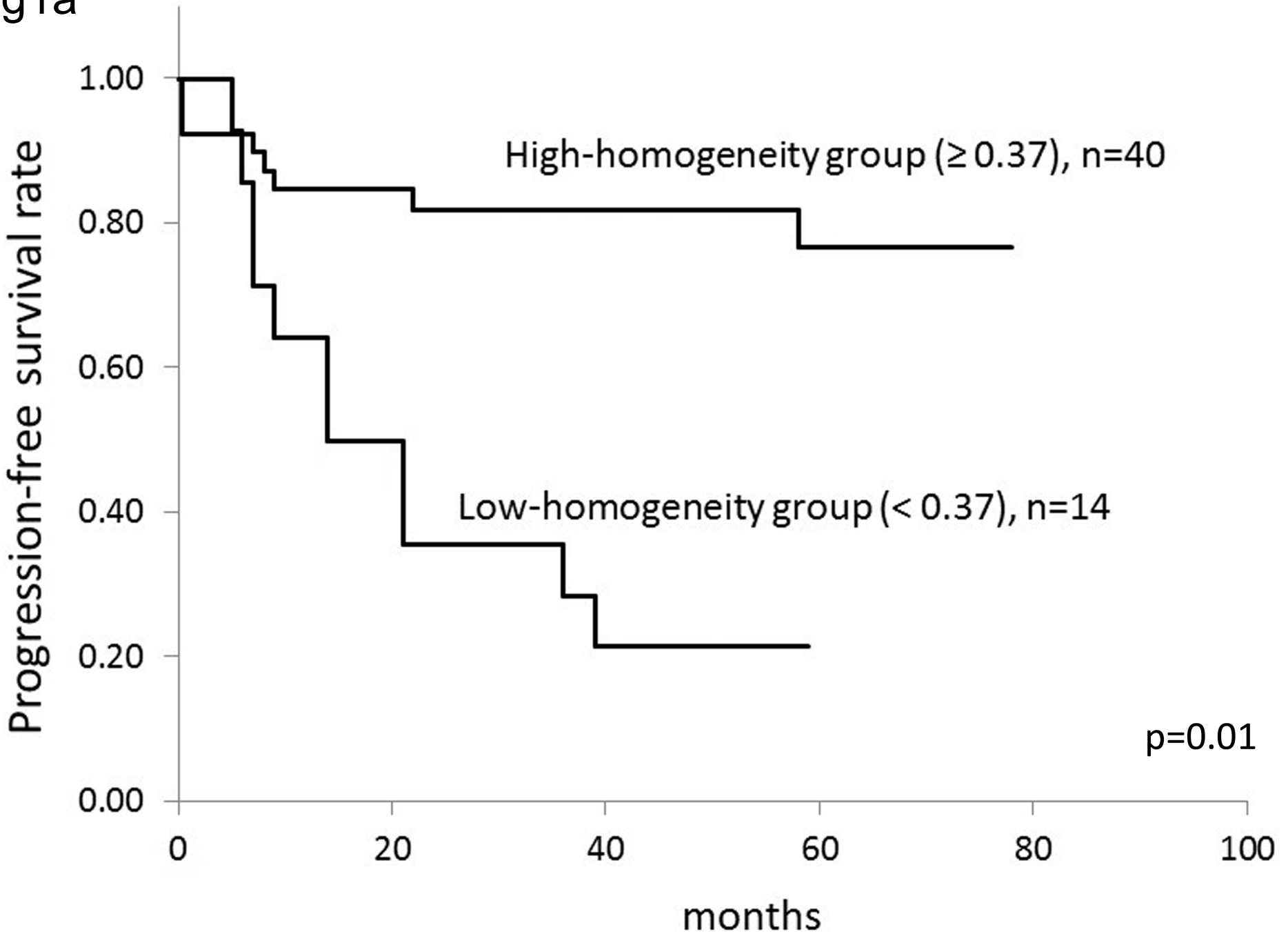
1.00
0.80
0.60
0.40
0.20
0.00
Progression-free survival rate
High-homogeneity group (≥ 0.37), n=40
Low-homogeneity group (< 0.37), n=14
p=0.01
0
20
40
60
80
100
months

Fig1b

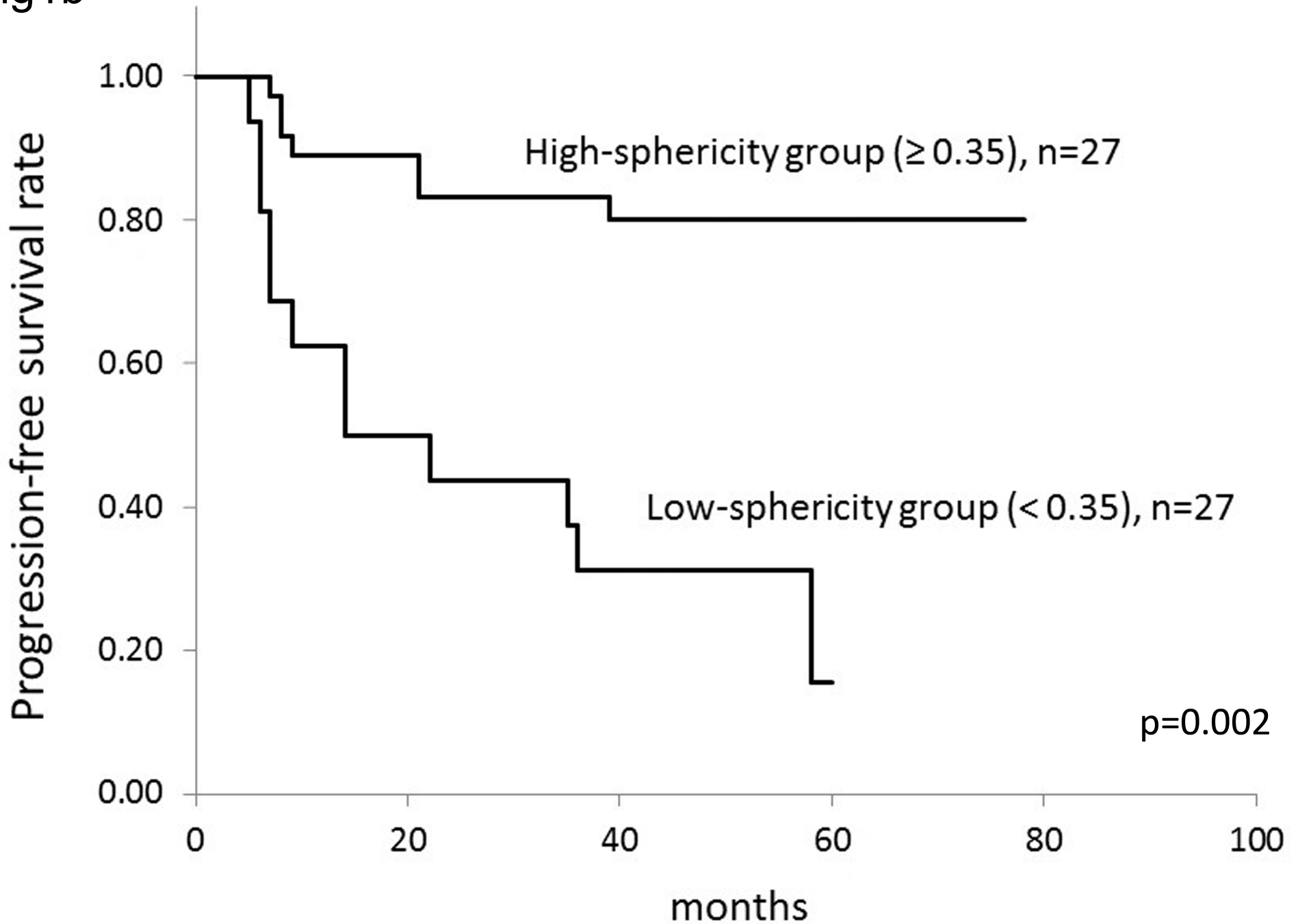
Progression-free survival rate
1.00
0.80
0.60
0.40
0.20
0.00
0
20
40
60
80
100
months
High-sphericity group (≥ 0.35), n=27
Low-sphericity group (< 0.35), n=27
p=0.002

Fig1c

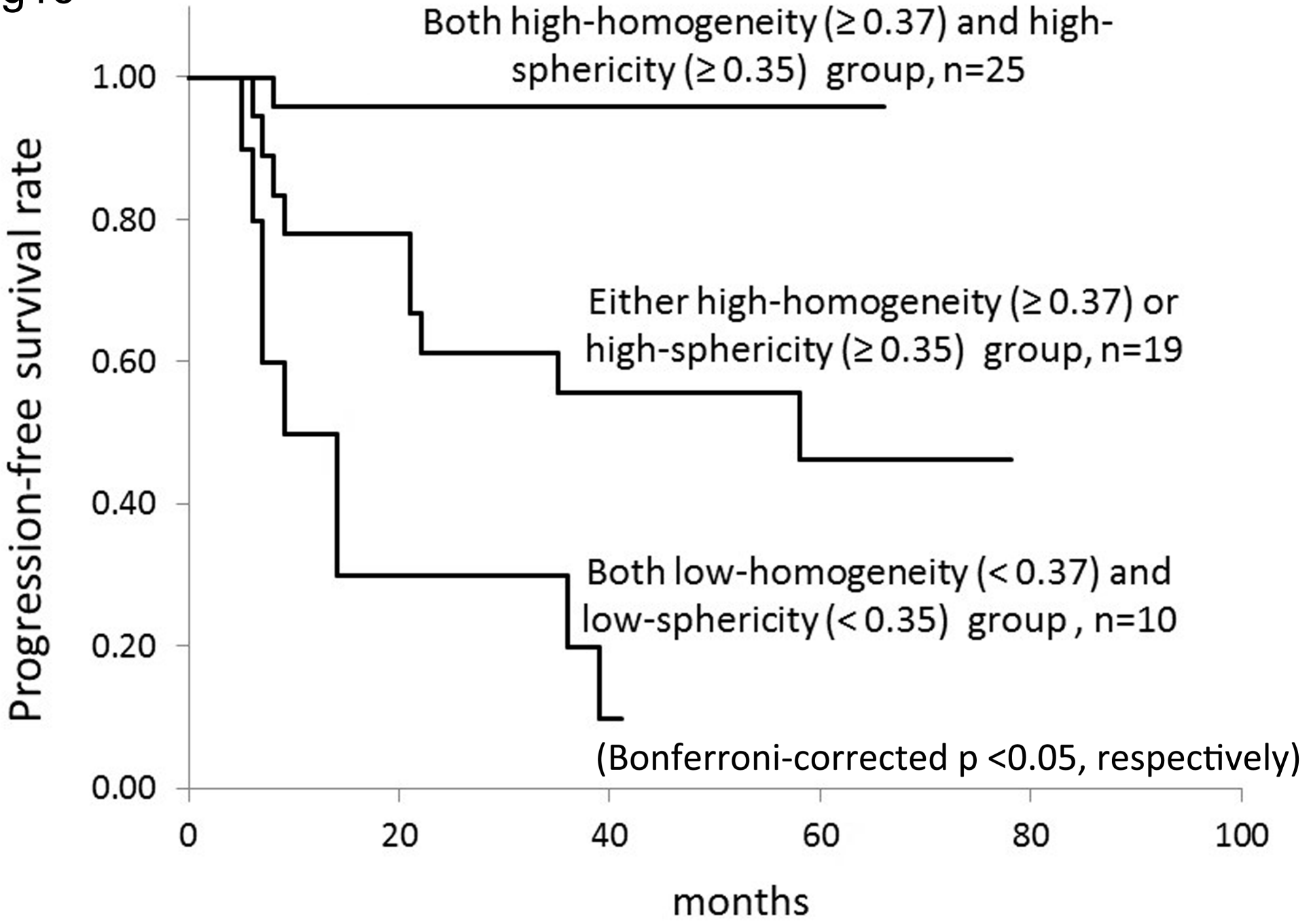
Both high-homogeneity (≥ 0.37) and high-sphericity (≥ 0.35) group, n=25
Either high-homogeneity (≥ 0.37) or high-sphericity (≥ 0.35) group, n=19
Both low-homogeneity (< 0.37) and low-sphericity (< 0.35) group , n=10
(Bonferroni-corrected p <0.05, respectively)
Progression-free survival rate
1.00
0.80
0.60
0.40
0.20
0.00
0
20
40
60
80
100
months